



Investigations of the Interaction Mechanism Between Orphenadrine Hydrochloride and Bovine Serum Albumin by Spectroscopic and Voltammetric Techniques

Naveen M. Gokavi^{1,3} · Sharanappa T. Nandibewoor¹ · Jayant I. Gowda²

Received: 28 January 2023 / Accepted: 3 March 2023 / Published online: 28 March 2023

© The Author(s), under exclusive licence to Springer Science+Business Media, LLC, part of Springer Nature 2023

Abstract

The interaction of orphenadrine hydrochloride (ORD) with the model protein, bovine serum albumin (BSA), was investigated using a variety of spectroscopic techniques such as steady-state fluorescence, ultraviolet–visible, Fourier transform infrared, 3-D spectroscopy, and electrochemical methods under physiological conditions. Stern–Volmer plots were used to calculate fluorescence quenching at various temperatures. The findings point to a static quenching mechanism between ORD and BSA. At various reaction times, the binding sites (n) and binding constants (K) of ORD to BSA were recorded. Thermodynamic parameters ΔH^0 , ΔS^0 and ΔG^0 between ORD and BSA were calculated and reported. The average binding distance (r) between the donor (BSA) and acceptor (ORD) molecules was predicted using Förster's theory. Three-dimensional fluorescence spectra, Fourier transform infrared spectra, and synchronous fluorescence studies all supported the alternations in protein structure following the interaction with ORD. A displacement study using site probes such as warfarin, ibuprofen, and digitoxin confirmed ORD binding at Sudlow's site I of BSA. The effect of common metal ions such as Cu^{2+} , Ni^{2+} , Ca^{2+} , Co^{2+} , and Zn^{2+} on binding constant values was investigated and reported.

Keywords Orphenadrine hydrochloride · Bovine serum albumin · Fluorescence · 3D spectra · Voltammetry

Introduction

Serum albumins are the most abundant protein found in a wide range of organisms in circulatory systems. They make a significant contribution to the control of osmotic blood

Highlights

- Present work reports the interaction of orphenadrine hydrochloride with bovine serum albumin.
- Fluorescence results revealed the presence of static quenching mechanism.
- Changes in confirmation and micro-environment of BSA were confirmed by Synchronous fluorescence spectrometry and 3D fluorescence spectra.
- Electrochemical data showed the intercalative mode of binding between BSA and ORD.

✉ Jayant I. Gowda
jayantgowda4@gmail.com

¹ P. G. Department of Studies in Chemistry, Karnatak University, Dharwad, Karnataka 580003, India

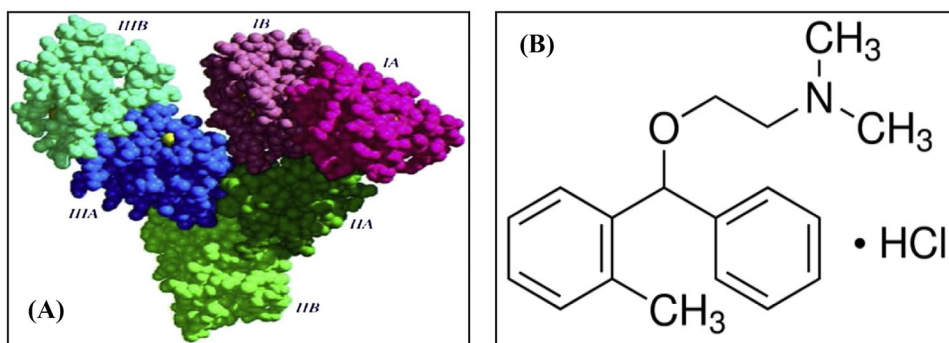
² Department of Chemistry, BLDEA's Commerce, BHS Arts and TGP Science College, Jamkhandi, Karnataka 587301, India

³ Department of Chemistry, Karnatak Science College, Dharwad, Karnataka 580001, India

pressure. Because the structure of bovine serum albumin (BSA) (Scheme 1A) is similar to that of human serum albumin (HSA) [1], extensive research has been conducted. BSA is involved in the metabolism of numerous compounds, including amino acids, fatty acids, drug molecules, and pharmaceutical samples [2–5]. They also contribute to the transport and distribution of the above mentioned molecules. The efficiency of many drugs depends on their ability to bind to proteins. The displacement of drugs from their binding sites may alter the distribution, metabolism, pharmacological action, and excretion of the displaced drug. Hence, it is essential to study in detail the interactions of drugs with different proteins, which has become an important research field in life sciences, clinical medicine, and chemistry.

Understanding the deeper levels of protein functionality, particularly in relation to their binding to ligands, can provide valuable structural and mechanical data for drug development purposes [6–8]. Proteins are considered the backbone of cellular processes, and clarifying the natural mechanisms of associated forces during binding processes can aid in the development of more effective drugs for medical applications. Protein-drug interactions play a fundamental role in pharmacokinetics, pharmacodynamics, clearance, efficiency, and toxicity of drug compounds

Scheme 1 Structure of **A** Bovine Serum Albumin (BSA) and **B** Orphenadrine hydrochloride (ORD)



in vivo [9–11]. This undeniable fact highlights the importance of studying protein–drug interactions in drug development.

Orphenadrine hydrochloride (N,N-dimethyl-2-(o-methyl-alpha-phenylbenzyloxy) ethylamine hydrochloride, Scheme 1B) (ORD) is a widely used anticholinergic drug. This ethanolamine antihistamine class of drug is used to treat central nervous system (CNS) disorders [12]. This medication was found to be effective in the treatment of painful muscle spasms as well as Parkinson's disease. ORD is widely used in psychiatric medicine to prevent and control extrapyramidal side effects caused by tranquilizers like phenothiazines. It is structurally similar to the non-opioid analgesic nefopam [13], as well as other Parkinson's disease medications such as benzotropine and trihexyphenidyl.

Fluorescence emission spectroscopy and UV–visible absorption spectroscopy are useful tools for understanding the complexities of chemical and biological systems. They use chemicals in low concentrations, particularly serum albumin. Under physiological conditions, these techniques exhibit high sensitivity, rapid analysis, and ease of study [14]. Nuclear magnetic resonance (NMR) spectroscopy [15], Fourier transform infrared spectroscopy [16], high performance liquid chromatography (HPLC) [17], affinity chromatography [18], and equilibrium dialysis [19] are other common techniques. To determine the dissociation constant of the drug–protein complex, for example, a longer analysis time and higher protein concentrations are required. Hence, the interaction of ORD with BSA was studied under physiological conditions using multi-spectroscopic techniques such as fluorescence, UV–visible absorption, and Fourier transform infrared (FT-IR) spectroscopy and voltammetry to determine the affinity of ORD with BSA and investigate the binding mechanism of the ORD–BSA system as well as the thermodynamics of their interaction.

Materials and Methods

Reagents and Chemicals

Orphenadrine hydrochloride (ORD), an anticholinergic drug, was purchased from Sigma Aldrich and used exactly as prescribed. SD fine-chem. limited provided bovine serum

albumin (BSA) (Fraction V), which was stored at 2 to 8 °C until use. The stock solutions were prepared using a phosphate buffer solution with the desired pH. The study's other chemicals and reagents were all analytical reagent grade. Throughout the project, deionized water was used.

Instrumentation

Fluorescence spectra were recorded on a Hitachi spectrofluorometer Model F-2000(RF-5301 PC, Tokyo, Japan) equipped with a 150W Xenon lamp, a 1.0 cm quartz cell and thermostatic cuvette holder. A single beam CARY 50-BIO UV–visible Spectrophotometer (Victoria, Australia), with a slit width of 5 nm was used to record absorption spectra of Drug–BSA system. FT-IR spectra were recorded on a Thermo Nicolet-5700 FT-IR spectrometer (Waltham, MA) accessed with a germanium attenuated total reflection (ATR) accessory, a XT-KBr beam splitter and a DTGS KBr detector. Fluorescence spectrometer having Chronos BH-ISS technology was used for lifetime measurements. Binding study through voltammetry was employed with electrochemical analyzer CHI-630D (CH Instruments Inc., USA) with a conventional three-electrode system. An Elico pH meter (Elico Ltd., India) was used to check and adjust pH of the solution.

The absorbance of ORD at higher concentration introduces the inner filter effect (IFE) that decreases the emission intensity of BSA, hence interfering with the quenching process; intensities were corrected to decrease the IFE according to the following equation. To eliminate the influence of the IFE, a common inherent problem in many fluorimetric procedures, fluorescence intensity was corrected by the following relationship [20].

$$F_{\text{Cor}} = F_{\text{Obs}} 10^{\frac{A_{\text{Exc}} + A_{\text{Emi}}}{2}}$$

Procedures

Fluorescence Quenching Study

For quenching study between protein–drug, concentrations of BSA protein was fixed at 1.6 μM and the concentrations

of drug was varied in the range of 0–15.0 μM . Fluorescence spectra were recorded at three different temperatures (288, 298 and 308 K) in the range of 280–550 nm upon excitation at 296 nm.

Life Time Measurements

The fluorescence decay of BSA was carried out in presence and absence of increasing concentration of ORD. The excitation and emission wavelength of BSA was fixed at 296 nm and 340 nm respectively. The concentration of protein, BSA, was fixed at 1.6 μM and that of ORD was varied from 0–1.6 μM in phosphate buffer solution of pH 7.4 at 298 K.

Absorption Measurements

The UV–visible measurements were carried out in presence and absence of drug ORD at fixed concentration of BSA. The selected range was 240–600 nm. The procedure was carried by fixing the BSA concentration at 1.6 μM and varying the ORD concentration from 1.6 to 16.6 μM in the presence of phosphate buffer at 298 K.

FT-IR Measurements

The FT-IR measurements of BSA in the presence and absence of ORD were made in the range 1200–1800 cm^{-1} . BSA and ORD concentrations were fixed at 1.6 μM in the presence of phosphate buffer at 298 K.

Synchronous Fluorescence Measurements

Synchronous fluorescence of ORD-BSA was measured by increasing concentrations of ORD (0–15.0 μM) and keeping BSA concentration (1.6 μM) constant by setting $\Delta\lambda = 15$ nm and $\Delta\lambda = 60$ nm ($\Delta\lambda = \lambda_{\text{ex}} - \lambda_{\text{em}}$). When $\Delta\lambda = 15$ nm, the spectrum characteristic of protein tyrosine residues were observed and when $\Delta\lambda = 60$ nm, the spectrum characteristic of protein tryptophan residues were observed.

3D Fluorescence Measurements

3D fluorescence spectra were recorded under the following conditions: excitation wavelength in the range of 260–380 nm and emission wavelength in the range of 200–600 nm at an interval of 10 nm with other parameters were just the same as that of fluorescence quenching spectra ($C_{\text{BSA}} = 1.6 \mu\text{M}$ and $C_{\text{ORD}} = 15.0 \mu\text{M}$).

Binding Studies

Fluorescence spectra of ORD (0–15.0 μM) with BSA in presence of probes viz., warfarin, ibuprofen and digitoxin were recorded in the range of 300–550 nm upon excitation at 296 nm. The BSA concentration and respective probes were fixed at 1.6 μM .

Effect of Some Metal Ions

The fluorescence spectra of ORD-BSA system were recorded in presence of some common metal ions viz., Cu^{2+} , Ni^{2+} , Ca^{2+} , Co^{2+} and Zn^{2+} at 298 K. For this ORD concentration was varied from 0–15.0 μM with fixed concentration of BSA and respective metal (1.6 μM) ions in the range of 300–550 nm upon excitation at 296 nm.

Cyclic Voltammetric Measurements

Using CHI-630 D electrochemical analyzer cyclic voltammograms were recorded by varying concentrations of ORD from 1.6 μM to 8.3 μM in absence and presence of 1.6 μM BSA concentrations. Throughout study pH of the PBS was 7.4, the system scan rate was 100 mVs^{-1} and concentration of BSA was fixed.

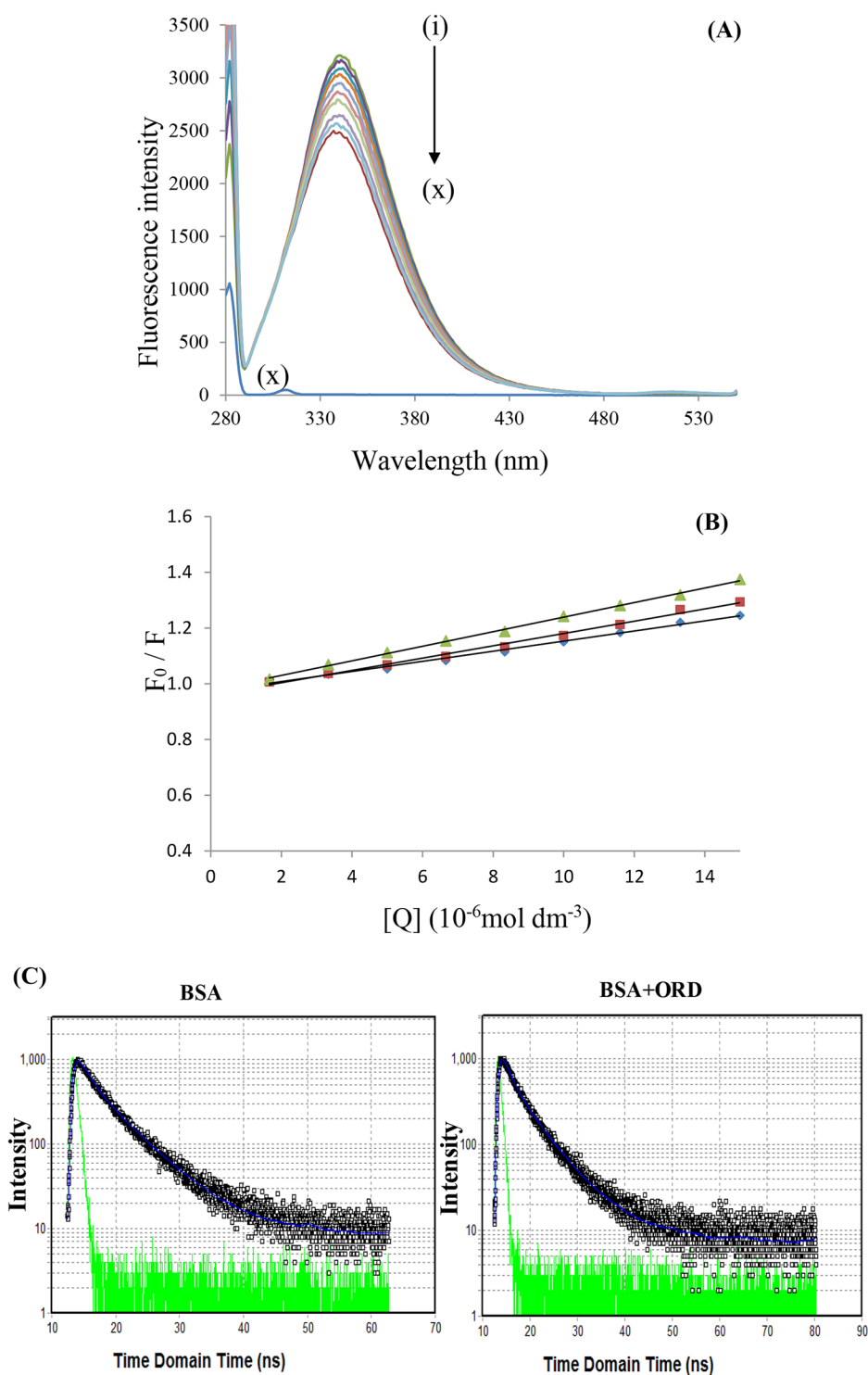
Results and Discussion

Fluorescence Quenching (FQ) Mechanism and Life Time Measurement Studies

The intrinsic fluorescence intensity of BSA was compared to the fluorescence spectra recorded in the presence and absence of the drug ORD to determine conformational changes. The effect of drug (ORD) on BSA fluorescence intensity is shown in Fig. 1A. The addition of ORD to a fixed concentration of BSA resulted in a decrease in fluorescence signal, as shown in fluorescence spectra. This suggests that the microenvironment around the BSA chromophore has changed. From Fig. 1A, the maximum wavelength of BSA was shifted from 340 to 336 nm after the addition of ORD. This small blue shift in maximum emission wavelength confirms that the protein chromophore was placed in a more hydrophobic environment after the addition of drug ORD [21].

Fluorescence quenching (FQ) can be dynamic or static for the interaction. Dynamic type quenching results if collisions occur between the fluorophore and quencher. When the formation of a ground-state complex between the fluorophore and quencher was observed, static quenching was observed

Fig. 1 a Fluorescence spectra of BSA in the presence of ORD. (i) 0 μM , (ii) 1.6 μM , (iii) 3.3 μM , (iv) 5.0 μM , (v) 6.6 μM , (vi) 8.3 μM , (vii) 10.0 μM , (viii) 11.6 μM , (ix) 13.3 μM , (x) 15.0 μM . Concentration of BSA was fixed at 1.6 μM . (x) is the fluorescence spectra of phosphate buffer. **b** The Stern–Volmer plots for quenching of BSA with ORD at 308 K (\blacktriangle), 298 K (\blacksquare), and 288 K (\blacklozenge). **c** Time-resolved fluorescence decay for lifetime measurement spectra of BSA and BSA + ORD system



[22]. By analysing fluorescence quenching data using equations, the Stern–Volmer investigation aids in predicting the possible type of fluorescence quenching mechanism [23].

$$F_0/F = 1 + K_{SV} [Q] = 1 + k_q \tau_0 [Q] \quad (1)$$

where F_0 is the intensity of the fluorescence in the absence of a quencher and F is the intensity of the fluorescence in the presence of a quencher. According to a plot of F_0/F against $[Q]$ with linear regression, the Stern–Volmer quenching constant, or K_{SV} , was determined (Fig. 1B). The fluorophore's

Table 1 Stern–Volmer quenching constants (K_{SV}), the quenching rate constant (k_q) and the effective quenching constant (K_a) for the interaction of ORD with BSA at 288, 298 and 308 K

System	T (K)	K_{SV} ($\text{dm}^3 \text{mol}^{-1}$)	k_q ($\text{dm}^3 \text{mol}^{-1} \text{s}^{-1}$)	K_a ($\text{dm}^3 \text{mol}^{-1}$)
BSA + ORD	288	2.61×10^4	2.61×10^{12}	3.86×10^4
	298	2.21×10^4	2.21×10^{12}	3.45×10^4
	308	1.81×10^4	1.81×10^{12}	3.01×10^4

average lifetime (τ_0) without a quencher is 10^{-8} s, and $[Q]$ is the quencher's concentration. K_q is the biomolecule's quenching rate constant. Stern–Volmer quenching constant K_{SV} is listed in Table 1 and has an inverse relationship with temperature. The value of k_q exceeds the biomolecule's limiting diffusion constant ($2.0 \times 10^{10} \text{ dm}^3 \text{ mol}^{-1} \text{ s}^{-1}$) [24]. These findings support the existence of a static quenching mechanism between BSA and ORD [25]. Additional analysis of the fluorescence data was performed using modified Stern–Volmer [26] Eq. (2):

$$F_0/\Delta F = F_0/F_0 - F = 1/f_a K_a [Q] + 1/f_a \quad (2)$$

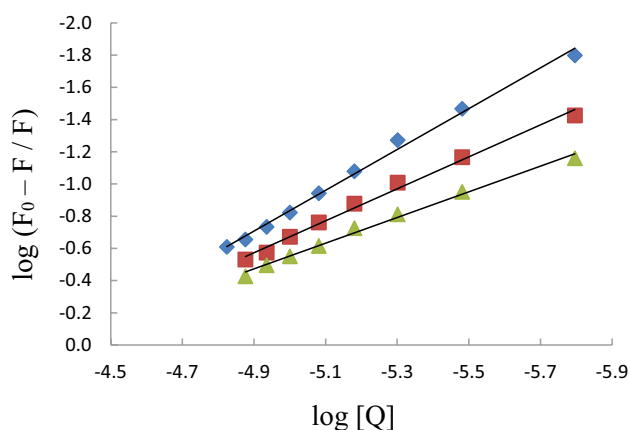
In this context, ΔF refers to the difference in fluorescence between the presence and absence of the quencher at concentration $[Q]$. f_a is called as fraction of available fluorescence. K_a serves as the effective binding constant for accessible fluorophores. At three distinct temperatures, the appropriate effective binding constants are listed in Table 1 for each temperature. The trend of K_a dropping as temperature rise indicates a static quenching mechanism. The life times of BSA and BSA + ORD were also examined in order to verify the static quenching mechanism, and the results are presented in Fig. 1C. The life times of BSA and BSA + ORD are 5.61 ± 0.05 for BSA and 5.63 ± 0.03 for BSA + ORD, respectively. According to the literature, these minor variations showed that the static type of quenching mechanism was responsible for the quenching of BSA by ORD [27].

Binding Constant and Number of Binding Sites

It is assumed that small drug molecules independently bind to a set of equivalent sites on macromolecules. The binding constant (K) and number of binding sites (n) for ORD-BSA system can be calculated using the equation given below [28]:

$$\log (F_0 - F/F) = \log K + n \log [Q] \quad (3)$$

where n and K stand for the number of binding sites and the binding constant. With the help of the $\log (F_0 - F/F)$ vs $\log [Q]$ plot, it is possible to estimate the values of n and K . This plot yielded a straight line with an intercept on the Y-axis equal to $\log K$ and a slope equal to n (Fig. 2). Table 2 provided a list of the values of K and n . There is just one

**Fig. 2** The plot of $\log(F_0 - F)/F$ versus $\log[Q]$ for quenching of BSA by ORD at 288 K (◆), 298 K (■) and 308 K (▲) $[ORD] = 0\text{--}15.0 \mu\text{M}$; $[BSA] = 1.6 \mu\text{M}$

binding site for ORD in BSA, based on the binding constant value (n), which is close to 1. Hence, ORD most likely binds to the hydrophobic pocket located in subdomain IIA; that is to say, Trp-214 is near or within the binding site [29]. As the temperature increases, the binding site values decrease, possibly because of the higher population of ORD in its ground state. This is because when ORD and BSA form a ground state complex, the population of ORD in the ground state is greater at lower temperatures compared to higher temperatures. The decrease in binding constant value with rising temperature may be brought about by decrease in stability of the complex ORD-BSA [30]. The static quenching mechanism discovered during the interaction of ORD and BSA exhibits behaviour similar to this one. The ground-state complex that develops between fluorophores and a quencher is what causes the static quenching.

Thermodynamic Analysis

Hydrophobic force, electrostatic contacts, van der Waals interactions, and hydrogen bonding are only a few of the potential forces that could interact with a large drug molecule. Predicting the types of forces acting between a medication and a protein is made easier by knowing the values of enthalpy change (ΔH^0) and entropy change (ΔS^0). The vant Hoff's Eq. (4) is used to compute ΔH^0 and ΔS^0 :

$$\log K = -\Delta H^0/2.303RT + \Delta S^0/2.303R \quad (4)$$

In Eq. (4), R is the universal gas constant, and K is the binding constant ($\text{dm}^3 \text{mol}^{-1}$) at the corresponding temperature ($8.314 \text{ J K}^{-1} \text{ mol}^{-1}$). The enthalpy change (ΔH^0) during the quenching process can be calculated using the slope and entropy change (ΔS^0) can be calculated with the help of intercept of a $\log K$ against $1/T$ plot (Fig. 3), respectively.

Table 2 Thermodynamic parameters of BSA+ORD system

System	T (K)	K (dm ³ mol ⁻¹)	n	ΔH ⁰ (kJmol ⁻¹)	ΔS ⁰ (J K ⁻¹ mol ⁻¹)	ΔG ⁰ (kJ mol ⁻¹)
BSA+ORD	288	3.16×10 ⁵	1.20			-30.1
	298	0.19×10 ⁵	0.99	-157.8	-505.8	-25.4
	308	0.03×10 ⁵	0.80			-19.9

K is the binding constant, n is the number of binding sites, ΔH⁰ is the enthalpy change, ΔS⁰ is the entropy change and ΔG⁰ is the free energy change

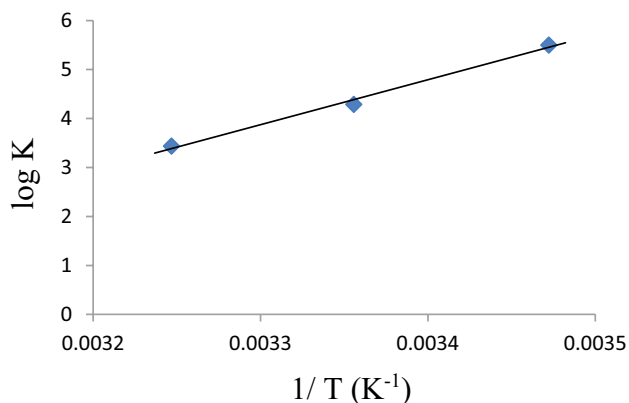
Then, as illustrated in Eq. (5), the free energy change (ΔG⁰) is calculated using the Gibbs–Helmholtz relationship:

$$\Delta G^0 = \Delta H^0 - T\Delta S^0 \quad (5)$$

According to Table 2, the van der Waals force and hydrogen bonds play a part in the interaction between ORD and BSA [31]. This is indicated by the negative values of enthalpy change and entropy change. The negative values of free energy (ΔG⁰) show that the binding process is spontaneous. The formation of the ORD-BSA complex is enthalpy-favourable but entropy-unfavourable, according to thermodynamic data.

Fluorescence Resonance Energy Transfer (FRET) Between ORD and BSA

Förster's theory of molecular resonance energy transfer was used to analyse the efficiency of energy transmission [32]. According to this theory, energy transfer may also occur by direct contact between the donor and acceptor. By this non-radiative theory, the energy transfer effect between acceptor and donor is related not only to the distance between them, but also on the critical energy transfer distance (R₀) and the efficiency of energy transfer (E). The extent of energy transfer between ORD and BSA is confirmed by the significant overlap in Fig. 4 between the

**Fig. 3** van't Hoff curve for the interaction of BSA with ORD

fluorescence and absorption spectra of ORD and BSA. Equation (6) is used to calculate the value of E:

$$E = 1 - \frac{F}{F_0} = \frac{R_0^6}{R_0^6 + r^6} \quad (6)$$

where F₀ and F denote the fluorescence intensities of BSA in the absence and presence of ORD. R₀ is the critical distance when the efficiency of transfer energy is 50%, and r is the binding distance between acceptor and donor. R₀⁶ can be calculated as

$$R_0^6 = 8.8 \times 10^{-25} \times k^2 N^{-4} \Phi J \quad (7)$$

where φ is the fluorescence quantum yield of the donor, k² is the spatial orientation factor of the dipole, N is the refractive index of the medium, and J is the overlap integral of the fluorescence emission spectrum of the donor with the absorption spectrum of the acceptor and is given by

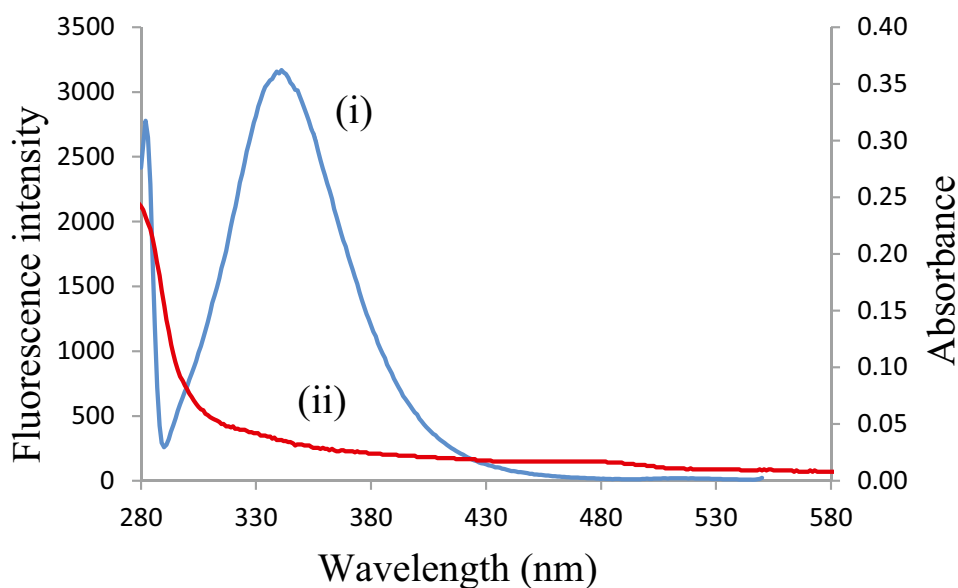
$$J = \frac{\sum F(\lambda)\epsilon(\lambda)\lambda^4\Delta\lambda}{\sum F(\lambda)\Delta\lambda} \quad (8)$$

where F(λ) is the fluorescence intensity of the donor at wavelength λ and ε(λ) is the acceptor's molar absorption coefficient at this wavelength. The overlap integral J in Eq. (8) can be calculated by integrating the spectrum. The value of J was calculated to be 8.0×10⁻¹⁴ cm³/L/mol. Using the values of k²=2/3, N=1.336 and φ=0.15 [33], the values of R₀, r and E were found to be 1.35 nm, 2.50 nm and 0.006, respectively. For energy transfer, an essential criterion is that the distance between the donor and acceptor must be within 2–8 nm. The results clearly showed that energy transfer from BSA to ORD occurred with a high probability [34].

Absorption Spectroscopic Studies

Figure 5 depicted the BSA absorbance spectrum (curve i). BSA displayed a noticeable absorption peak at about 288 nm, which was caused by π-π* electronic transitions in the phenyl group of the Phe, Trp, and Tyr residues [35]. The absorbance of Trp and Tyr depend on the microenvironment of their chromophores, and their shift to either side of wavelength range (i.e. red or blue) depends upon the polarity of surrounding.

Fig. 4 Overlap of (i) fluorescence spectrum of BSA and (ii) absorbance spectrum of ORD. ($C_{\text{BSA}} = C_{\text{ORD}} = 1.6 \mu\text{M}$)



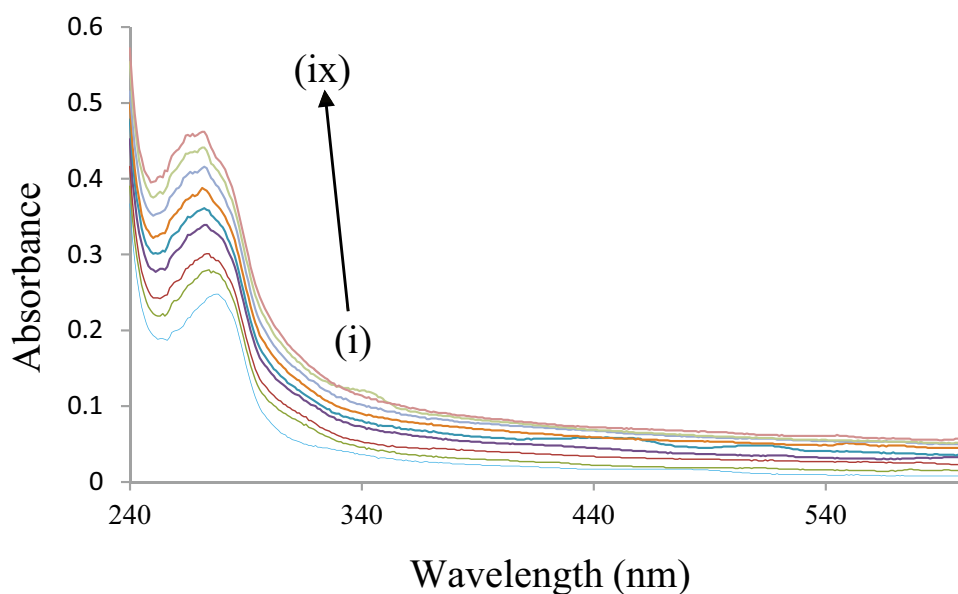
While the peptide groups of the protein main chain absorb light in the far-UV range (180 nm–230 nm). Various side chains, including those of Trp, Phe, Tyr, His, Cys, Met, and Arg (in the descending order), make contributions to the absorption in this wavelength range. There was a change in the absorbance of BSA around 288 nm (Fig. 5) in the presence of ORD which suggests that micro environment of aromatic amino acids, particularly tryptophan residues (Trp 213 and Trp 131) have been affected marginally upon binding with ORD. It was also observed that there was a slight blue shift in wavelength maxima of BSA UV–Vis absorption spectra in the presence of ORD. The blue shift in the wavelength maxima clearly suggested an increase in the hydrophobicity in the microenvironment

around tryptophan residues [36]. Therefore, change in absorbance, blue shift in wavelength maxima clearly suggested binding interaction between BSA and ORD.

FT-IR Spectral Studies

The structural alterations of BSA after the addition of ORD can be confirmed by FT-IR spectroscopy and are shown in Fig. 6A, B. The stretching frequencies in the regions $1500\text{--}1600 \text{ cm}^{-1}$ (mainly C=O stretch) and $1500\text{--}1600 \text{ cm}^{-1}$ (C–N stretch coupled with N–H bending mode) provide information about amide I and amide II conformation in the native and unfolded states, respectively [37–39].

Fig. 5 Absorbance spectra of ORD–BSA system. ORD concentration for ORD–BSA system was at (i) 0 μM , (ii) 1.6 μM , (iii) 3.3 μM , (iv) 5.0 μM , (v) 6.6 μM , (vi) 8.3 μM , (vii) 10.0 μM , (viii) 11.6 μM , and (ix) 13.3 μM . ($C_{\text{BSA}} = 1.6 \mu\text{M}$)



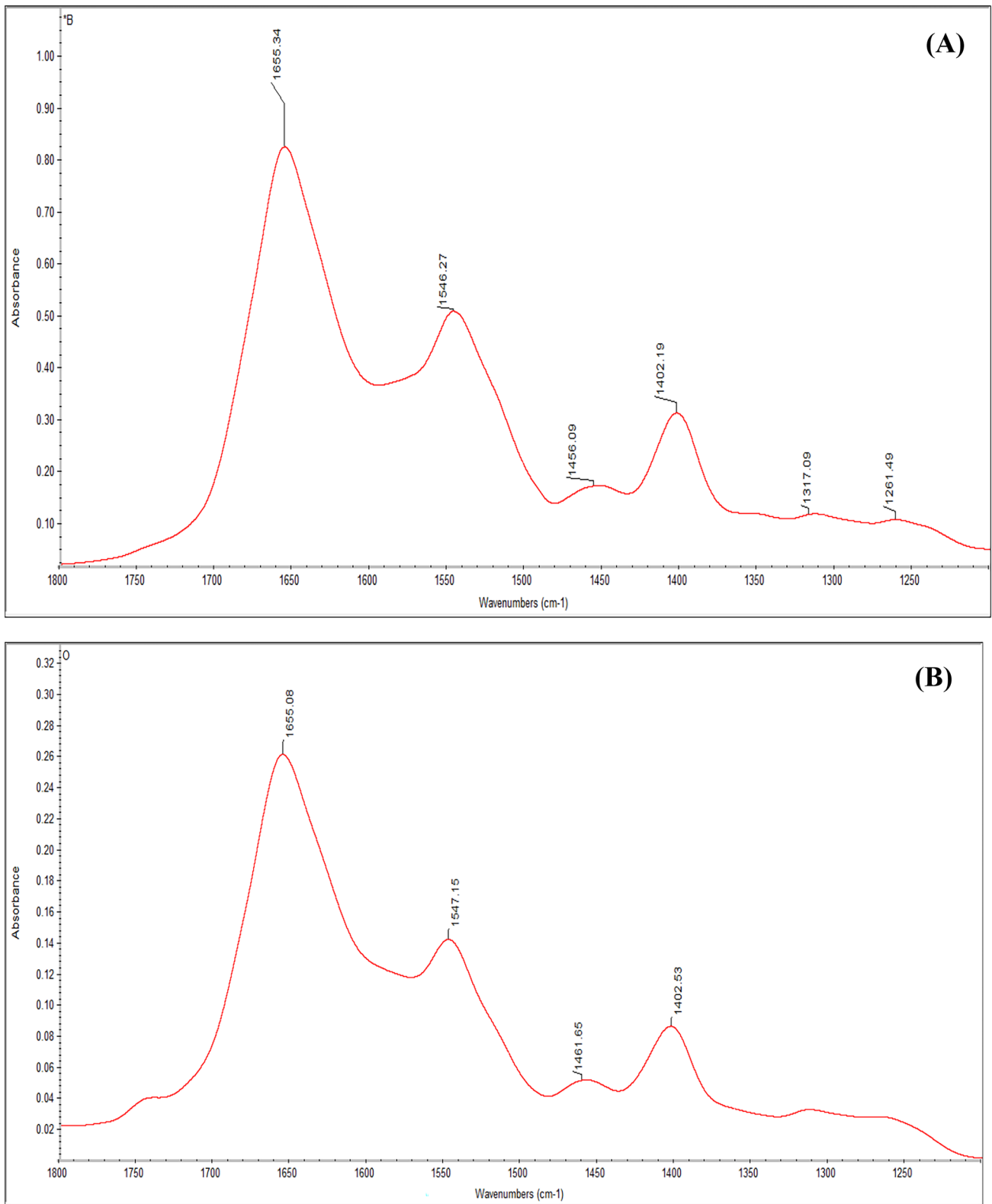


Fig. 6 FTIR spectrum **A** BSA and **B** BSA-ORD system. ($C_{\text{BSA}} = C_{\text{ORD}} = 1.6 \mu\text{M}$)

It was observed that the peak positions of the amide I and amide II bands remained unchanged, but the peak intensity of the amide I band was markedly decreased in comparison with the amide II band. This is due to a shift in the proportion of proteins α -helix structures [40]. As a result, we can confirm that the α -helix content of BSA was reduced after binding with ORD. The BSA-ORD complex formation is through the rearrangement of the polypeptide carbonyl hydrogen bonding network followed by reduction of the α -helical structure of proteins. Hence, the secondary structures of BSA were changed by the interaction of ORD with BSA.

Synchronous Fluorescence Spectrometry (SFS)

To validate the FT-IR results, synchronous fluorescence spectrometry of protein (BSA) was performed before and after drug addition. Figure 7A, B show synchronous fluorescence spectrometry scans at 15 and 60 nm. The characteristics of tyrosine (Tyr) or tryptophan (Trp) residues were revealed when the difference between the excitation and emission wavelengths was 15 nm or 60 nm [41]. According to Fig. 7A, B, the maximum emission wavelength for Tyr residue ($\Delta\lambda = 15$ nm) remained unchanged, whereas the maximum emission wavelength for Trp residue represents a weaker red shift ($\Delta\lambda = 60$ nm). These findings show that the polarity around the Trp residues changes and the hydrophobicity of BSA decreases after conformational changes. This could be due to changes in the residue microenvironment caused by ORD insertion.

3D Fluorescence Spectrometry

3-D fluorescence spectra are now important in fluorescence analysis techniques [42]. It provides detailed information about the protein's conformational changes. The 3 D fluorescence spectra of the BSA (A) and ORD + BSA (B) systems are shown in Fig. 8. Peak '1' represents the Rayleigh scattering peak ($\lambda_{ex} = \lambda_{em}$), and strong peak '2' describes the spectral properties of Trp and Tyr residues on proteins. The maximum emission wavelength of the peak was changed after the addition of ORD, as shown in Fig. 8B, and the contour map displayed a bird's eye view of the fluorescence spectra.

Effect of Some Metal Ions

Human blood contains common metal ions that are widely distributed and may be able to bind with proteins. This may have an effect on drug binding to albumin. As a result, we looked into how some common bivalent metal ions affected drug binding to albumin. The binding constants

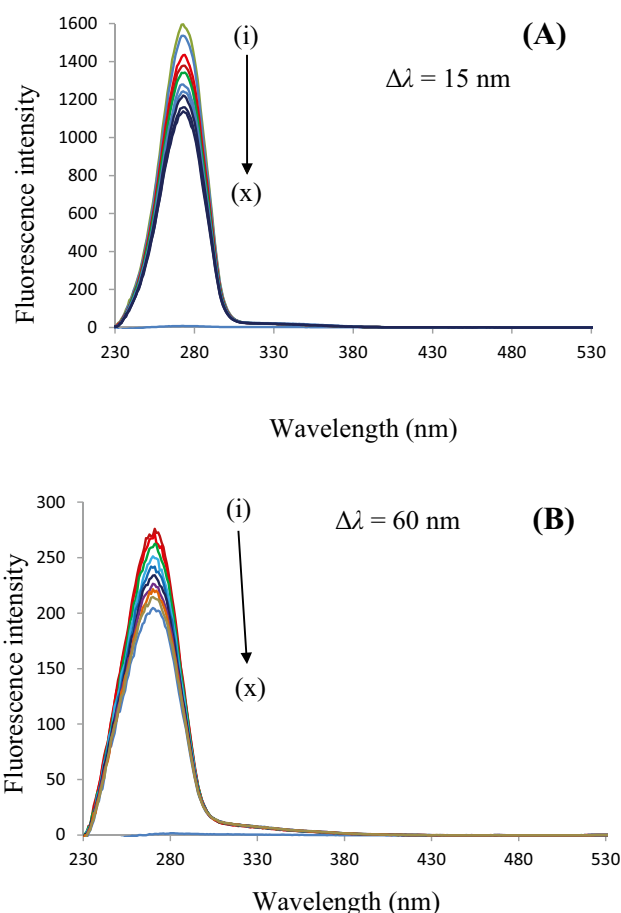


Fig. 7 Synchronous fluorescence spectrum of BSA-ORD ($T = 298$ K, pH 7.40), (A) $\Delta\lambda = 15$ nm (B) $\Delta\lambda = 60$ nm. Concentration of ORD: (i) 0 μ M, (ii) 1.6 μ M, (iii) 3.3 μ M, (iv) 5.0 μ M, (v) 6.6 μ M, (vi) 8.3 μ M, (vii) 10.0 μ M, (viii) 11.6 μ M, (ix) 13.3 μ M, (x) 15.0 μ M. The concentration of BSA was fixed at 1.6 μ M

of ORD-BSA were determined and listed in Table 3 in the presence of various metal ions such as Cu^{2+} , Ni^{2+} , Ca^{2+} , Co^{2+} , and Zn^{2+} . It was discovered that the binding constant of ORD-BSA decreased in the presence of certain common bivalent ions. This indicates that the drug and the bivalent metal ion are competing for the same site in the protein. This leads to displacement of the drug from the binding site of the protein and an increase in the free drug concentration in blood plasma. These effects impose a higher dosage of the drug to achieve the preferred therapeutic effect [43].

Site Probe Studies

To investigate the distinct binding site for ORD on BSA, Sudlow et al. [44] and Sjöholm et al. [45] used site-specific ligands: warfarin, ibuprofen, and digitoxin for sites I, II, and III, respectively. Individual emission spectra of BSA-ORD and ternary mixtures of BSA-site probe-ORD were recorded

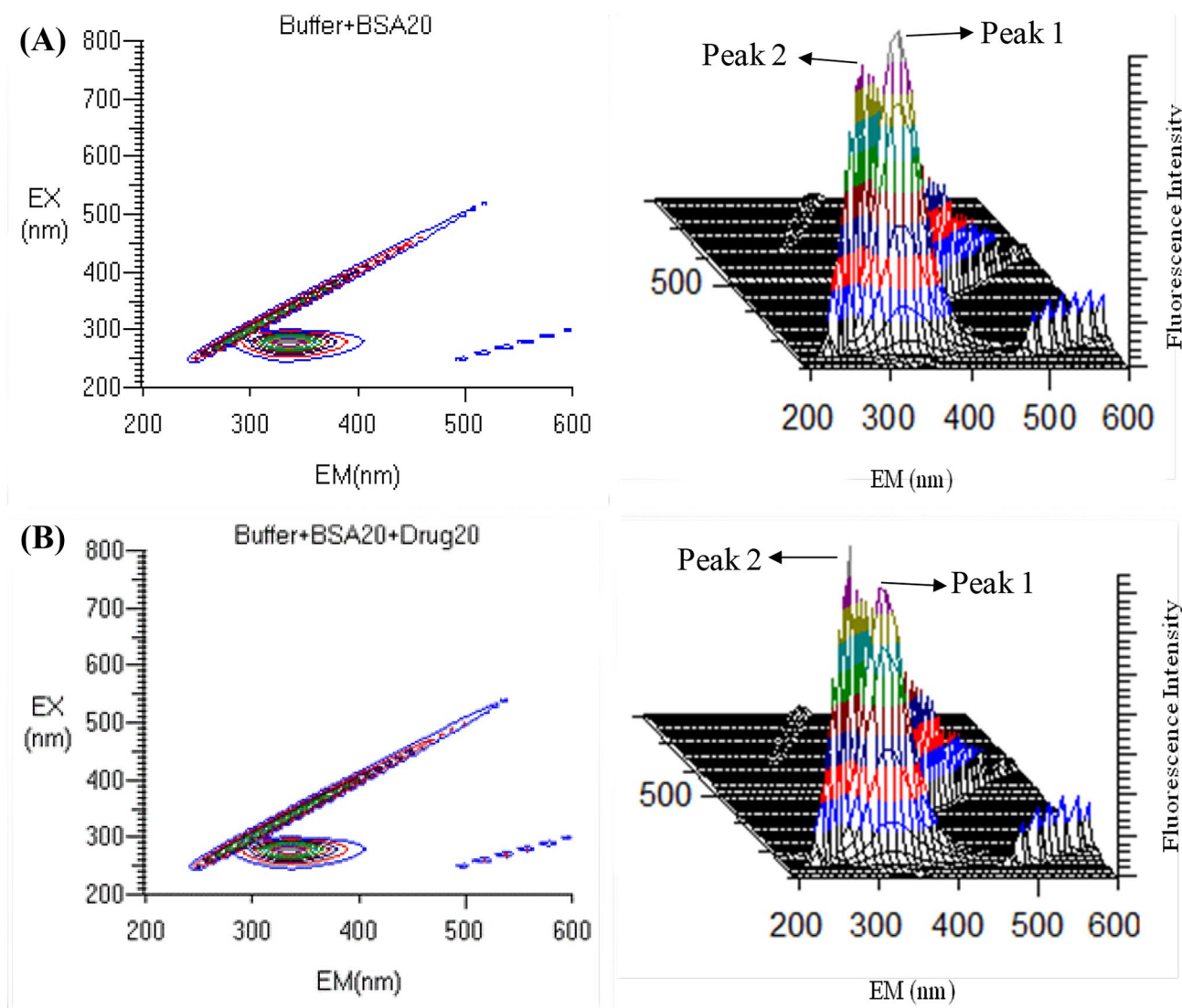


Fig. 8 Three-dimensional excitation–emission matrix spectral profile **A** BSA, **B** BSA + ORD system

for this purpose, and the resulting binding constant values in the presence of warfarin, ibuprofen, and digitoxin were calculated using Eq. (3) (Table 4). The results show that the binding constant of the BSA-ORD system decreased significantly

with the addition of warfarin while remaining nearly constant in the presence of ibuprofen and digitoxin. As a result, the binding site of ORD was primarily located within BSA site I (subdomain IIA).

Table 3 Effect of common metal ions on binding constant (K) of BSA + ORD system

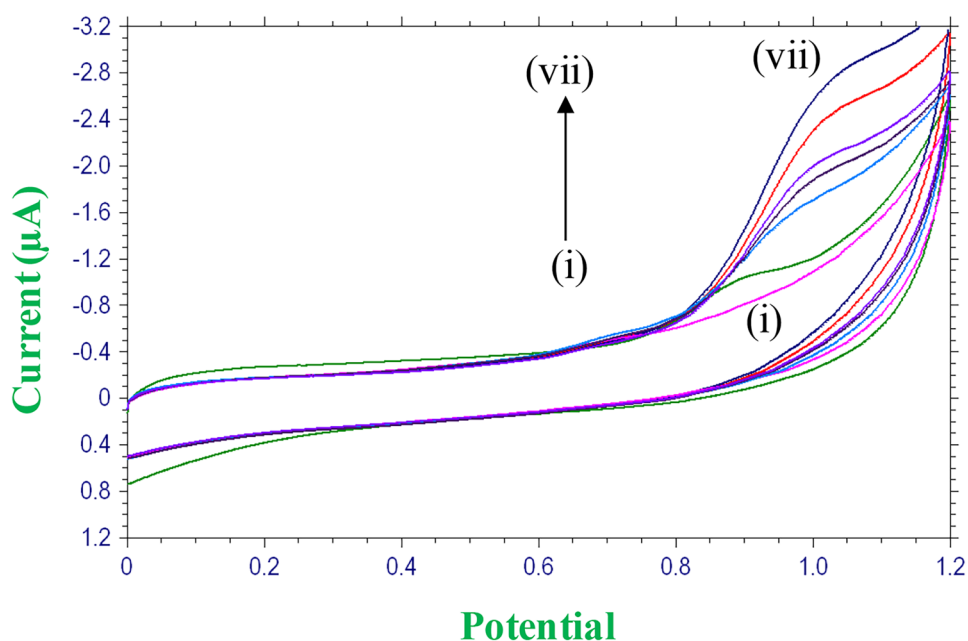
System	K ($\text{dm}^3 \text{mol}^{-1}$)
BSA + ORD	0.19×10^5
BSA + Cu^{2+} + ORD	0.43×10^4
BSA + Ni^{2+} + ORD	0.85×10^4
BSA + Ca^{2+} + ORD	0.76×10^4
BSA + Co^{2+} + ORD	0.29×10^4
BSA + Zn^{2+} + ORD	0.14×10^4

Table 4 Comparison of binding constant of BSA + ORD system with site probes (Warfarin, ibuprofen and digitoxin)

System	K ($\text{dm}^3 \text{mol}^{-1}$)	n
BSA + ORD	0.19×10^5	0.99
BSA + Warfarin + ORD	0.20×10^4	0.82
BSA + Ibuprofen + ORD	0.90×10^4	0.90
BSA + Digitoxin + ORD	0.82×10^4	0.95

K is the binding constant and n is the number of binding sites

Fig. 9 Cyclic voltammogram of ORD in the presence of BSA (1.6 μM) with different concentration at (iii) 1.6 μM , (iv) 3.3 μM , (v) 5.0 μM , (vi) 6.6 μM , and (vii) 8.3 μM of ORD ($T=298\text{ K}$, $\text{pH } 7.40$) at a scan rate of 100 mV/s where as curves represent voltammogram of (i) BSA (1.6 μM) and (ii) ORD (1.6 μM)



Cyclic Voltammetric Studies

The cyclic voltammograms of ORD in the absence and presence of BSA were recorded at a scan rate of 100 mV/s in the potential range of 0–1.2 V (Fig. 9). In the presence of BSA, the voltammogram of ORD revealed an oxidation peak at 0.9136 V, which was shifted to a positive potential of 0.9891 V with an increase in current. Furthermore, the peak current increases with increasing amounts of ORD in the presence of BSA (from curve (iii) to curve (vii)). One of the following two factors could account for such an observation: (i) The nonconductive BSA could prevent electron transfer from the ORD, or (ii) the resulting BSA + ORD complex was electrochemically inactive. When electron transfer is blocked, the current should decrease (relative to the clean electrode), but no peak shift is expected [46]. As a result, the observed shift in peak potential was attributed to the formation of the BSA + ORD complex via intercalative binding [47]. Thus, the electrochemical studies proposed the intercalative mode of binding between the ORD and BSA based on the spectroscopic results.

Conclusion

BSA-ORD interaction was investigated using steady-state fluorescence, UV–visible, Fourier transform infrared, and cyclic voltammetry techniques. The results showed that ORD quenched the intrinsic fluorescence of BSA via a static quenching mechanism. The role of van der Waals force and hydrogen bonds in the stabilisation of the BSA + ORD complex was revealed by thermodynamic

analysis. Synchronous fluorescence spectrometry and 3D fluorescence spectra confirm that there is a change in the confirmation and microenvironment of BSA when it interacts with ORD. The electrochemical data revealed that BSA and ORD bind in an intercalative mode. This type of research into the interaction of BSA and ORD would be useful in the pharmaceutical industry, life sciences, and clinical medicine.

Contributions

Dr. Naveen M. Gokavi carried out Literature Survey, material preparation, data collection. Dr. Jayant I. Gowda involved in Data analysis and preparation of draft manuscript. Prof. S. T. Nandibewoor finalized the drafted manuscript. All authors read and approved the final manuscript.

Acknowledgements One of the author Naveen M. Gokavi thanks Karnatak University Dharwad, Dharwad for the award of UGC-UPE fellowship.

Data Availability The authors confirm that the data supporting the findings of this study are available within the article.

Declarations

Ethics Approval Ethical approval was not required because no human or animal was involved for conducting present study.

Consent to Participate Informed consent was obtained from all individual participants included in the study.

Consent to Publish The authors affirm that present study does not contain any human research data.

Competing Interests The authors have no relevant financial or non-financial interests to disclose.

References

- Papadopoulou A, Green RJ, Frazier RA (2005) Interaction of flavonoids with bovine serum albumin: A fluorescence quenching study. *J Agric Food Chem* 53:158–163
- Kumar CV, Buranaprapuk A (1999) Tuning the selectivity of protein photocleavage: Spectroscopic studies and photochemical studies. *J Am Chem Soc* 121:4262–4270
- He XM, Carter DC (1992) Atomic structure and chemistry of human serum albumin. *Nature* 358:209–215
- Feng XZ, Lin Z, Yang LJ, Wang C, Bai CL (1998) Investigation of the interaction between acridine orange and bovine serum albumin. *Talanta* 47:1223–1229
- Bolattin MB, Nandibewoor ST, Chimatadar SA (2016) Biomolecular interaction study of hydralazine with bovine serum albumin and effect of β -cyclodextrin on binding by fluorescence, 3D, synchronous, CD, and Raman spectroscopic methods. *J Mol Recognit* 29:308–317
- Moghadam SK, Ezazi-Toroghi S, Vatanparast MK, Jouyaeian P, Mokaberi P, Yazdani H, Tehranizadeh ZA, Saberi MR, Chamani J (2022) Novel perspective into the interaction behavior study of the cyaniding with human serum albumin-holo transferring complex: Spectroscopic, calorimetric and molecular modelling approaches. *J Mol Liq* 356:119042
- Sharifi-Rad A, Mehrzad J, Darroudi M, Saberi MR, Chamani J (2021) Oil-in-water nanoemulsions comprising Berberine in olive oil: Biological activities, binding mechanisms to human serum albumin or holotransferrin, and QMMD simulations. *J Biomol Struct Dyn* 39:1029–1043
- Marjani N, Dareini M, Lotfabad MA, Pejhan M, Mokaberi P, Tehranizadeh ZA, Saberi MR, Chamani J (2022) Evaluation of the binding effect and cytotoxicity assay of 2-Ethyl-5-(4-methylphenyl) pyrimidopyrazoleophthalazinetrione on calf thymus DNA: spectroscopic, calorimetric, and molecular dynamics approaches. *Luminescence* 37:310–322
- Maheri H, Hashemzadeh F, Shakibapour N, Kamelniya E, Nikouei BM, Mokaberi P, Chamani J (2022) Glucokinase activity enhancement by cellulose nanocrystals isolated from jujube seed: A novel perspective for type II diabetes mellitus treatment (In vitro). *J Mol Str* 1269:133803
- Hosseinzadeh M, Nikjoo S, Zare N, Delavar D, Beigoli S, Chamani J (2019) Characterization of the structural changes of human serum albumin upon interaction with single-walled and multi-walled carbon nanotubes: spectroscopic and molecular modeling approaches. *Res Chem Intermed* 45:401–423
- Chamani J, Moosavi-Movahedi AA, Hakimelahi GH (2005) Structural changes in β -lactoglobulin by conjugation with three different kinds of carboxymethylcyclodextrins. *Thermochim Acta* 432:106–111
- Withers NJ, Chauhan AJ, Holgate ST (1996) Pulmonary and critical care pharmacology and therapeutics. McGraw-Hill, New York
- Fernández-Sánchez MT, Díaz-Trelles R, Groppetti A, Manfredi B, Brini AT, Biella G, Sotgiu ML, Novelli A (2002) Nefopam, an analogue of orphenadrine, protects against both NMDA receptor-dependent and independent veratridine-induced neurotoxicity. *Amino Acids* 23:31–36
- Ashoka S, Seetharamappa J, Kandagal PB, Shaikh SMT (2006) Investigation of the interaction between trazodone hydrochloride and bovine serum albumin. *J Luminescence* 121:179–186
- Price WS, Ge NH, Hong LZ, Hwang LP (1993) Characterization of chloride ion binding to human serum albumin using chlorine NMR null point spectral analysis. *J Am Chem Soc* 115:1095–1105
- Tang D, Li HJ, Li P, Wen XD, Qian ZM (2008) Interaction of bioactive components caffeoylquinic acid derivatives in Chinese medicines with bovine serum albumin. *Chem Pharm Bull* 56:360–365
- Wang HL, Zou HF, Zhang YK (1997) Determination of drug-protein interaction by combined microdialysis and high performance liquid chromatography. *Chromatographia* 44:205–208
- Sjöholm I, Ljungstedt I (1973) Studies on the tryptophan and drug binding properties of human serum albumin fragments by affinity chromatography and circular dichroism measurements. *J Biol Chem* 248:8434–8441
- Shen XC, Liang H, Guo JH, Songh C, He XW, Yuan YZ (2003) Studies on the interaction between Ag^+ and human serum albumin. *J Inorg Biochem* 95:124–130
- Taheri R, Hamzkanlu N, Rezvani Y, Niroumand S, Samandar F, Amiri-Tehranizadeh Z, Saberi MR, Chamani J (2022) Exploring the HSA/DNA/lung cancer cells binding behavior of p-Synephrine, a naturally occurring phenyl ethanol amine with anti-adipogenic activity: multi spectroscopic, molecular dynamic and cellular approaches. *J Mol Liq* 368:120826
- Tian J, Liu J, Hub Z, Chen X (2005) Interaction of wogonin with bovine serum albumin. *Bioorg Med Chem* 13:4124–4129
- Lakowicz JR (1999) Principles of fluorescence spectroscopy. Kluwer Academic/Plenum Press, New York
- Lakowicz JR (2006) Principles of fluorescence spectroscopy, 3rd edn. Springer publications, New York, USA
- Lakowicz JR, Weber G (1973) Quenching of fluorescence by oxygen. A probe for structural fluctuations in macromolecules. *Biochemistry* 12:4161–4170
- Roy AS, Tripathy DR, Chatterjee A, Dasgupta S (2010) A spectroscopic study of the interaction of the antioxidant naringin with bovine serum albumin. *J Biophys Chem* 1:141–152
- Samari F, Shamsipur M, Hemmateenejad B, Samari T, Gharaghani S (2012) Investigation of the interaction between amodiaquine and human serum albumin by fluorescence spectroscopy and molecular modelling. *Eur J Med Chem* 54:255–263
- Huang S, Peng S, Zhu F, Lei X, Xiao Q, Su W, Liu Y, Huang C, Zhang L (2015) Multispectroscopic investigation of the interaction between two ruthenium(II) arene complexes of curcumin analogs and human serum albumin. *Biol Trace Elem Res* 169:189–203
- Ross PD, Subramanian S (1981) Thermodynamics of protein association reactions: forces contributing to the stability. *Biochemistry* 20:3096–3102
- Bi S, Song D, Tian Y, Zhou X, Liu Z, Zhang H (2005) Molecular spectroscopic study on the interaction of tetracyclines with serum albumins. *Spectrochim. Acta A Mol Biomol Spectrosc* 61:629–636
- Cui FL, Fan J, Li J-P, Hu Z-D (2004) Interactions between 1-benzoyl-4-p-chlorophenyl thiosemicarbazide and serum albumin: investigation by fluorescence spectroscopy. *Bioorg Med Chem* 12:151–157
- Shaikh SMT, Seetharamappa J, Kandagal PB, Manjunatha DH, Ashoka S (2007) Spectroscopic investigations on the mechanism of interaction of bioactive dye with serum albumin. *Dyes Pigm* 74:665–671
- Förster T (1996) Modern Quantum Chemistry. Academic Press, New York
- Cyrl L, Earl JK, Sperry WM (1961) Biochemist's Handbook, E and F.N. Spon: London
- Valeur B, Brochon JC (1999) New trends in fluorescence spectroscopy, 6th edn. Springer Press, Berlin
- Ding F, Diao JX, Sun Y, Sun Y (2012) Bioevaluation of human serum albumin-hesperidin bioconjugate: Insight into protein vector function and conformation. *J Agric Food Chem* 60:7218–7228

36. Pathak M, Mishra R, Agarwala PK, Ojha H, Singh B, Singh A, Kukreti S (2016) Binding of ethyl pyruvate to bovine serum albumin: Calorimetric, spectroscopic and molecular docking studies. *Thermochim Acta* 633:140–148
37. Zhang G, Que Q, Pan J, Guo J (2008) Study of the interaction between icariin and human serum albumin by fluorescence spectroscopy. *J Mol Struct* 881:132–138
38. Azimi O, Emami Z, Salari H, Chamani J (2011) Probing the interaction of human serum albumin with norfloxacin in the presence of high frequency electromagnetic fields: fluorescence spectroscopy and circular dichroism investigations. *Molecules* 16:9792–9818
39. Ding F, Li N, Han B, Liu F, Zhang L, Sun Y (2009) The binding of C.I. acid red to human serum albumin: Determination of binding mechanism and binding site using fluorescence spectroscopy. *Dyes Pigm* 83:249–257
40. Yuan T, Weljie AM, Vogel HJ (1998) Tryptophan fluorescence quenching by methionine and selenomethionine residues of calmodulin: Orientation of peptide and protein binding. *Biochemistry* 37:3187–3195
41. Yue YY, Zhang YH, Zhou L, Qin J, Chen XG (2008) In vitro study on the binding of herbicide glyphosate to human serum albumin by optical spectroscopy and molecular modelling. *J Photochem Photobiol B* 90:26–32
42. Miller JN (1979) Recent advances in molecular luminescence analysis. *Proc Anal Div Chem Soc* 16:203–208
43. Li Y, He WY, Liu JQ, Sheng FL, Hi ZD, Chen XG (2005) Binding of the bioactive component jatrorrhizine to human serum albumin. *Biochim Biophys Acta* 1722:15–21
44. Sudlow G, Birkett DJ, Wade DN (1976) Further characterization of specific drug binding sites on human serum albumin. *Mol Pharmacol* 12:1052–1061
45. Sjöholm I, Ekman B, Kober A, Pahlman IL, Seiving B, Sjödin T (1979) Binding of drugs to human serum albumin: XI. The specificity of three binding sites as studied with albumin immobilized in microparticles. *Mol Pharmacol* 16:767–777
46. Wang Y, Ni Y, Kokot S (2011) Voltammetric behaviour of complexation of salbutamol with calf thymus DNA and its analytical application. *Anal Biochem* 419:76–80
47. Carter MT, Rodriguez M, Bard AJ (1989) Voltammetric studies of the interaction of metal chelates with DNA. 2. Tris-chelated complexes of cobalt (III) and iron (II) with 1,10-phenanthroline and 2,2'-bipyridine. *J Am Chem Soc* 111:8901–8911

Publisher's Note Springer Nature remains neutral with regard to jurisdictional claims in published maps and institutional affiliations.

Springer Nature or its licensor (e.g. a society or other partner) holds exclusive rights to this article under a publishing agreement with the author(s) or other rightsholder(s); author self-archiving of the accepted manuscript version of this article is solely governed by the terms of such publishing agreement and applicable law.